# The Competing Chemical and Physical Effects of Transient Fuel Enrichment on Heavy Knock in an Optical Spark Ignition Engine

Hassan Vafamehr, Alasdair Cairns(*), Ojon Sampson, Mohammadmohsen Moslemin Koupaie

Division of Mechanical Engineering, Brunel University London, UB8 3PH, London, UK

(*) Corresponding author: alasdair.cairns@brunel.ac.uk, Tel: +44(0)1895 265175

## ABSTRACT

The work was concerned with improving understanding of the chemical and physical trade-offs when employing transient over-fuelling to control auto-ignition in gasoline spark ignition engines under knock intensities not usually tolerated in optical engines. The single cylinder engine used included full bore overhead optical access capable of withstanding unusually high in-cylinder pressures. Heavy knock was deliberately induced by adopting inlet air heating and a primary reference fuel blend of reduced octane rating. High-speed chemiluminescence imaging and simultaneous in-cylinder pressure data measurement were used to evaluate the combustion events. Under normal operation the engine was operated under port fuel injection with a stoichiometric air-fuel mixture. Multiple centred auto-ignition events were regularly observed, with knock intensities of up to ~30bar. Additional excess fuel was then introduced directly into the end-gas in short transient bursts. As the mass of excess fuel was progressively increased a trade-off was apparent, with knock intensity first increasing by up to 65% before lower unburned gas temperatures suppressed knock under extremely rich conditions. This trade-off is not usually observed during conventional low intensity knock suppression via over-fuelling and has been associated with the competing effects of reducing auto-ignition delay time and charge cooling/ratio of specific heats. Overall, the results demonstrate the risks in employing excess fuel to suppress knock deep within a heavy knocking combustion regime (potentially including a Super-Knock regime).

KEYWORDS: Optical, Auto-Ignition, Developing Detonation, Downsizing, Knock, Super-Knock

## 1. INTRODUCTION

Over the last few decades European automotive manufacturers have met fuel economy targets mainly through increased diesel sales. However, the efficient distillation of crude oil produces similar amounts of gasoline and diesel fuel and European passenger diesel sales have now approached saturated levels [1]. The recent "dieselgate" scandal surrounding diesel engine emissions has also tarnished the reputation of diesel engines for automotive applications. Overall, in the short-to-medium term it is necessary to improve the fuel consumption of the "cleaner" gasoline engine and in the longer term source sustainable alternatives to crude oil. Substitutes such as electric and hydrogen fuel cell vehicles, hybrid vehicles and biofuels are among the alternatives being investigated. However, significant challenges remain with respect to the sustainability of such technologies to meet global demand. For electric vehicles, relatively low energy and power densities and high production cost remain key barriers [2]. For biofuels, advanced fuel production techniques are still required to produce fuels in a near carbon-neutral manner with improved energy security and less reliance on feedstock [3-5].

One method for improving gasoline engine efficiency is engine downsizing, which is currently being widely adopted by automotive manufacturers. The basic principle is to reduce the capacity of the engine and hence enforce a larger proportion of operation to higher loads. As a result, under wider open throttle conditions the pumping losses are reduced for a given road-load requirement. In order to maintain adequate vehicle acceleration and top speed, the smaller engine must be pressure-charged and still produce acceptable transient response. Overall, for a large family-sized saloon car, it has been demonstrated that halving total engine capacity from a V6 2.4 litre to a three-cylinder 1.2 litre unit can reduce fuel consumption by ~25%, with vehicle performance maintained [6].

Such downsizing clearly yields significant part-load fuel consumption benefits, but significant challenges remain including problematic combustion. Downsizing (and “downspeeding” via longer gearing) enforces a considerable proportion of "real world" operation to the low speed/high load regime. Under such conditions the increased energy density of a highly pressure charged mixture leads to an increased tendency for the fuel and air to auto-ignite. The problem of auto-ignition is almost as old as the internal combustion engine itself [7] and still ultimately caps peak thermal efficiency in modern SI engines [8-10], being commonly avoided by selecting a lower compression ratio, retarding the spark timing and/or introducing excess fuel. Such auto-ignition has been established to be the result of exothermic centres, or "hot spots", leading to auto-ignition of the unburned charge ahead of the developing flame [11-13]; so-called end-gas auto-ignition. However, recent aggressively downsized research engines of very high specific output have additionally experienced pre-ignition combustion at low engine speeds and high loads (>15 bar BMEP). Previously pre-ignition was most commonly associated with higher engine speeds, when the components within the combustion chamber are typically at their hottest. Hence such pre-ignition was at first unexpected, arising below the auto-ignition temperature of the charge and occurring in a highly sporadic manner in short violent bursts in an "on-off" pattern, with sometimes tens of thousands of cycles in-between events [14].

This phenomenon, widely referred to as Low Speed Pre-Ignition (LSPI) and "Super-Knock", has been associated with low-to-moderate thermal gradients within the unburned charge leading to developing detonation events. Ultimately, this may produce multiple high frequency and intensity pressure waves within the cylinder that may interact and ultimately destroy the engine. The time to trigger the auto-ignition chemistry of a given mixture under known physical conditions provides a useful relative measure of the expected onset and intensity of such events. This auto-ignition delay period cannot be accurately measured directly in real engines due to the complex nature of the combustion process. The delay period is therefore typically estimated using simplified chemical

kinetic schemes [15-18] and/or empirical measurements obtained in idealised rapid compression machines or combustion chambers [19-22].

Researchers at Shell and the University of Leeds [23] have recently postulated that such Super-Knock events originate from a resonance between acoustic waves emitted by an auto-igniting hot spot and a reaction wave that propagates along negative temperature gradients in the fuel-air charge. The theory is based upon the assumption that the temperature gradient extends smoothly over sufficient length across the turbulent flow field. Subsequently, localised detonations may develop which are then able to violently ignite the remaining unburned charge in timescales of less than a millisecond. Ultimately, this can lead to catastrophic mechanical engine failure. Peters and co-workers [24, 25] extended this theory developed at Leeds/Shell to at least partially attribute the random nature of the events to the stochastic nature of the in-cylinder turbulence. However, some uncertainty still remains around the triggering of these events. The pre-ignition typically occurs well below the auto-ignition temperature of the bulk charge, considered to be indicative of a deflagration caused by an exothermic centre with the high temperature gradient across it [14, 26]. It has also been suggested that the auto-ignition might be caused by a localised volume of charge with particularly low auto-ignition temperature, such as an evaporating droplet of lubricant (or mixtures of fuel and oil due to wall impingement of a directly injected fuel spray). Such droplets, of relatively low octane number (and high cetane number), have been suggested to cause the formation of the deflagration site(s) leading to pre-ignition and Super-Knock. To this end Dahnz et al. [14] produced a simple pre-ignition model to qualify the effects of a low-octane droplet within the main (high-octane) charge. It was found that a region existed where, given sufficient droplet temperature, ignition could be initiated below the bulk auto-ignition temperature of the main charge. When developing their theory Kalghatghi and Bradley [23] used pressure data from real engine Super-Knock cycles to show that gas-phase pre-ignition of an evaporating lubricant droplet could be possible, assuming that the lubricant droplet was substantially more reactive than n-heptane. In

recent work by SouthWest Research Institute many lubricants were found to meet this condition [27].

With the complex nature of cyclic variations in SI engines influenced by varying turbulence, charge homogeneity, wall temperatures, deposit conditions, fuel and oil properties [13, 14, 25, 27, 28] it is quite probable that the stochastic pre-ignition event is caused by a combination of phenomena. However the theory of an increased likelihood of auto-ignition occurring due to suspended oil droplets has widely gained credibility. Amann et al. [27] found that, during a sequence of Super-Knock events in a multi-cylinder engine, the air-fuel ratio was significantly reduced compared to the calibrated air-fuel ratio. When extremely high intensity knocking combustion was artificially induced by intermittently advancing the spark timing, the same trend in air-fuel ratio was not observed. This observation was therefore attributed to the accumulation of lubricant during normal engine running and its subsequent release from the piston top-land crevice during Super-Knock events. In other recent work by some of the current authors [29], oil was deliberately directly injected into the charge of a full bore optical engine, with the transport properties of the lubricant indicated to have some effect on the likelihood of pre-ignition and knock occurring. These observations were in good agreement with those reported simultaneously elsewhere in a full metal engine by Wellings and co-workers using identical lubricant blends [30].

In existing spark ignition engines the onset of knock is sometimes avoided by running fuel-rich [31, 32], where the charge cooling properties and reduced ratio of specific heats suppresses the onset of knocking combustion. This is undertaken at the expense of poor fuel consumption and vastly increased tailpipe emissions (given the three-way catalyst is no longer effective). Nonetheless, the slightly rich combustion may help maximise full load output. In addition, excess fuel is also commonly utilised at higher speeds and loads to limit exhaust gas temperatures and protect the exhaust components. Such operation is clearly not sustainable, particularly in light of the real world driving cycles currently being proposed within the EU and elsewhere to cover a wider area of engine operation. Furthermore, questions remain over the consequences of rich operation during

Super-Knock in downsized spark ignition engines, where pre-ignition may lead to a sudden violent knocking event and the presence of excess fuel (and/or inappropriate fuel stratification) could be detrimental. The complexity is arguably further exacerbated by emerging future fuels, where a fuel such as ethanol with high sensitivity (i.e. relatively high RON but low MON) may help reduce the onset of knock [1, 33-35] but could theoretically exacerbate sporadic pre-ignition under certain conditions due to the increased pre-ignition tendency as indicated by the lower MON rating [36].

The currently reported work was therefore concerned with evaluating the effects of excess fuel when introduced under heavy knocking conditions as might be experienced in modern automotive gasoline engines. Prior optical studies of auto-ignition have provided useful insight into the physical triggers [37, 38] and chemical species [39, 40] involved in the auto-ignition processes and/or alternative fuel effects [41, 42]. These prior studies in optical engines have generally been restricted to relatively low in-cylinder pressures. An alternative approach is to adopt partial optical access [43], with higher gas pressures then tolerated but the location of the auto-ignition initiation uncertain. Elsewhere, others have attempted to adopt fibre optic [44] or high speed endoscopic [45] based detector systems in thermodynamic multi-cylinder engines. Such systems suffer from limited field of view and/or limited sensitivity in locating the light emission from the original auto-ignition site(s). The current approach was therefore intended to uniquely provide full bore optical measurements in order to gain further insight into the auto-ignition initiation and effects of the transient over-fuelling with high knock intensities.

## 2. Experimental Setup

### 2.1. Optical Engine

The experiments were undertaken in a customized single cylinder research engine including a unique optical arrangement. The bottom-end was based on a commercial Lister-Petter TS1 including full-bore overhead optical access and a semi-traditional poppet-valve valvetrain. The

engine has been designed with a special window mounting, including a large fused silica window mounted in a soft metallic sleeve (with a thin layer of special high temperature sealant between the silica and metal). The special mounting has been developed to withstand continuous peak in-cylinder pressures of up to 150bar. Otherwise the engine incorporated a flat piston crown, two inlet ports and was originally designed with two exhaust ports. To increase trapped residuals and help invoke knock, one of the exhaust valves was deactivated as previously reported by Dingle et al. [29] and illustrated in Figure 1. The recessed side mounted poppet valves helped achieve valve overlap without piston clash and maintain a compression ratio of 8.4:1 [29].

The engine was coupled to an eddy-current dynamometer with a maximum power absorption/supply of 10kW. Port fuelling was controlled via a Bosch EV6 PFI fuel injector regulated to 3bar gauge rail pressure. The PFI injector mounted in the intake port and had a 2-hole pattern forming a dual plume spray pattern targeted towards the intake valves. In addition, a production multi-hole direct fuel injector (Model Year 2006 VW Golf 1.4 TSI 125kW) was positioned in the side of the head as indicated in Figure 1. The targeting of this injector was previously verified using optical shadowgraph measurements by Dingle [29]. The rail pressures of the PFI and DI fuel systems were set to 3 bar and 65 bar gauge respectively. The injection timing for port fuel injection was fixed (with an end of injection at 400°bTDC firing) while the timing of the DI was varied. Throughout the tests the engine was fuelled using a “PRF75” blend (75% isooctane, 25% n-heptane), with high purity isooctane and n-heptane obtained from a chemical supplier and blended on a volumetric basis. The chemical properties of the reference fuels are provided in Appendix A. Otherwise, the ignition system included a NGK ER9EH 8mm spark plug connected to a Bosch P100T ignition coil. The full experimental setup is shown schematically in Appendix B. The high speed flame images were cyclically resolved allowing study of the evolution of the combustion events during individual cycles. An NAC MEMRECAM fx6000 high speed video camera, coupled to a DRS Hadland Model ILS3-11 image intensifier, was used to record all optical data. The camera was triggered at the same time as the DAQ to record images

simultaneously with the pressure and temperature data. The camera was set to record at 8000 frames per second (fps) at a resolution of 512 x 308 pixels (3 pixels per mm) meaning that the time-resolved images were acquired every 1.15 crank angle degrees. The optical equipment was attached to an optical table suspended over the dynamometer. A mirror positioned at 45° over the bore allowed the camera to capture the flame data via natural light imaging.

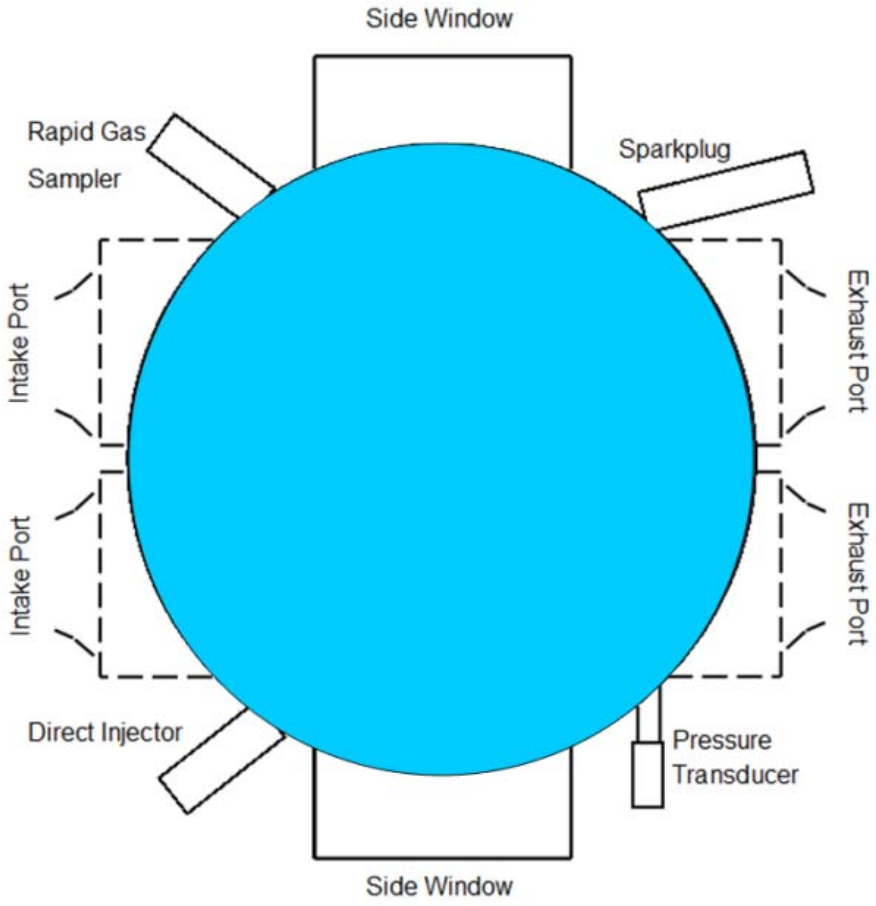


**Figure 1: Overhead view of the full bore window**

| Parameter (unit) | Value |
|---|---|
| Number of Cylinders | 1 |
| Compression Ratio | 8.4:1 |
| Stroke (mm) | 89 |
| Bore (mm) | 95 |
| Displacement (cc) | 631 |
| Con-rod Length (mm) | 165.16 |
| Valve Lift (mm) | 5 |
| Inlet Valve Openings/Closing ($^{o}$bTDC in degree) | 375/145 |
| Exhaust Valve opening/Closing ($^{o}$aTDC in degree) | 120/350 |

**Table 1 Key Engine Geometry**

### 2.2. Thermodynamic Analysis

A non-cooled AVL GH14DK pressure transducer was fitted in the cylinder head, with the face of the transducer mounted flush with the combustion chamber walls. The intake plenum pressure was also measured using a GEMS 1200 series CVD sensor. Both of these were recorded at four samples per crank angle degree via a digital shaft encoder, attached to the intake camshaft, and a Labview high-speed USB data-logging card. The engine operating temperatures were measured via a separate lower-speed card at 1Hz. Since the research engine was air-cooled, the cylinder head and liner temperatures were strictly monitored throughout the tests with two large stationary electric air fans positioned around the engine for improved temperature control. Cylinder head temperature measurement was undertaken at two locations: a) the DI injector tip and b) the exhaust valve bridge. The measurements obtained by both cards were collated and processed using an in-house MATLAB based system. The well-known Rassweiler and Withrow method [46] was used to determine the Mass Fraction Burned (MFB), which was considered adequate for the qualitative analysis intended. Thermodynamic results were averaged over 300 cycles but obtained in 100 cycle batches to minimise metal temperature variation effects in the air cooled unit. The average knock intensity was computed by filtering the raw pressure signal and calculating the average peak value over the full 300 cycles.

### 2.3. Engine Test Procedure

A fixed reference point was obtained by running the engine under normal non-knocking part-load operation until the cylinder head metal temperature reached 88°C. At this temperature knock was instantaneously induced by advancing the spark timing. After capturing the data, the engine was stopped, allowed to cool and the process repeated. This procedure kept the measured wall temperatures within a small range (<5°C peak-to-peak variation), which was necessary when considering knock in a qualitative manner with an engine setup lacking water cooling in the head. In a similar manner to the knock intensity calculations, the thermodynamic results were averaged over three sets of 100 cycles for each test condition. Table 2 below shows the engine test conditions used throughout the work. The sump oil temperature remained moderately low but fixed throughout testing (~40°C).

| **Parameter (unit)** | **Value** |
|---|---|
| Engine Speed (RPM) | 1200±5 |
| Relative AFR (λ)(PFI Only) | 1±0.01 |
| COV of IMEP (%) (PFI Only) | 5 |
| Inlet Pressure (bar) | 0.9±0.02 |
| Inlet Air Temperature ($^{o}$C) | 66±2 |
| Exhaust Bridge Temperature ($^{o}$C) | 130±2 |
| DI Tip Temperature ($^{o}$C) | 102±4 |
| Head Temperature ($^{o}$C) | 88±1 |

**Table 2 Engine Test Conditions**

## 3. Transient Direct Fuel Injection Results

Set out in Figure 2 are the cycle-by-cycle values of average knock intensity with and without additional direct fuel injection, with the Direct Injection Start of Injection (DI SOI) timing set to 60°bTDC firing and the DI pulse width set to 7ms. Under these conditions the overall relative air-to-fuel ratio increased from $\lambda$=1.0 to $\lambda$=0.66. The dashed line superimposed shows the activation signal sent to the DI injector. The average values of knock intensity (KI) before and after direct injection were 7.7bar and 0.48bar respectively. It can be seen that knock was largely suppressed and returned to similar levels when the fast over-fuelling was deactivated after ~30 cycles; albeit marginally lower in magnitude (KI ~6.3bar) which was associated with the lower peak gas temperatures during non-knocking combustion and differences in wall heat transfer. The differences in the in-cylinder pressure development are more apparent when observing the waterfall plot in Figure 3, which shows a cropped selection of cycles immediately before, during and after the over-fuelling event. Overall, the result verified the experimental setup, with the elimination of knock associated with the previously well reported charge cooling and ratio of specific heat effects of a relatively high amount of excess fuel introduced within the cylinder [31, 47].

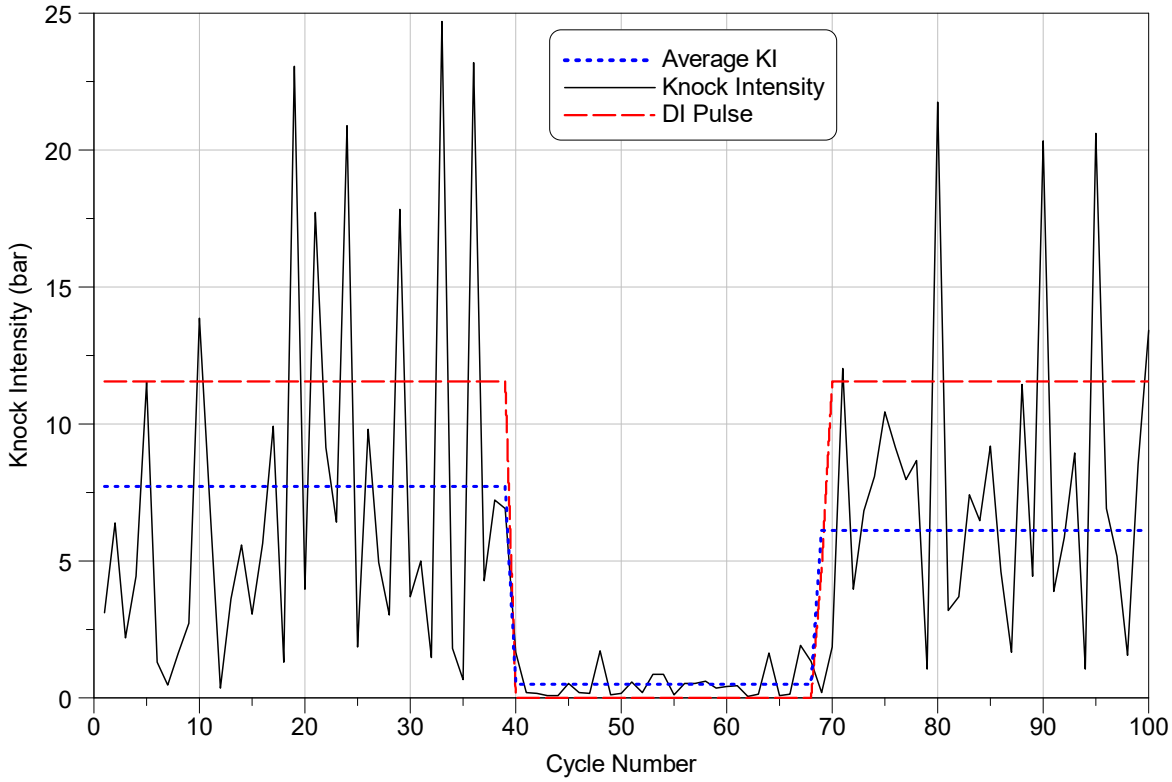


**Figure 2: Individual cycle average knock intensity versus engine cycle number before, during and after a transient over-fuelling event**

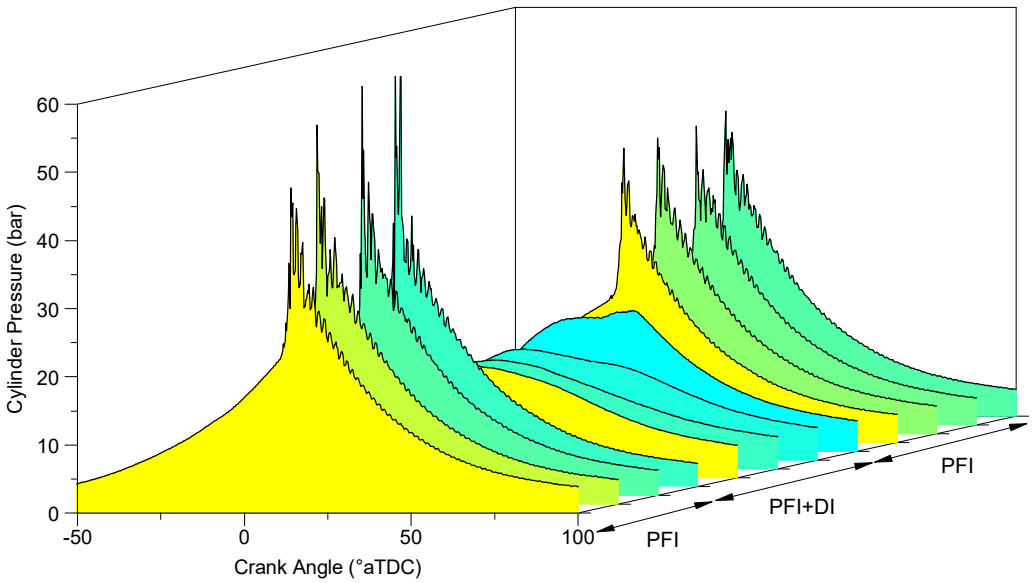


**Figure 3 Waterfall plot showing the differences in the in-cylinder pressure development before, during and after additional direct fuel injection**

### 3.1. Start of Injection Timing Sweep

A DI SOI timing sweep was undertaken to establish response to varying fuel stratification, as might be experienced during transient engine operation and/or advanced knock control in modern DI engines. Typically, after the exhaust valve closes, the earlier the injection timing the more homogeneous the fuel/air equivalent ratio field. However, it is also important to note that the mixture formation homogeneity, bulk fluid motion and turbulence intensity during the compression stroke can be strongly affected by the piston and the direct injection itself.

Throughout the sweep the DI fuel pressure was left fixed at 65bar. This left two variables; injection timing and additional fuel mass (injection pulse width). In initial work the pulse width was fixed to a relatively high value of 7ms (estimated to be an upper limit given the above result) and the SOI timing swept from 120° to 20°bTDC firing in intervals of 5° crank. The results are set out in Figure 4, where the solid black dots denote the value of average KI measured immediately prior to each DI

activation in PFI-only mode, included to show the consistency of the baseline knocking cases. The stars denote the average KI when the direct injection was activated. When the direct injection was advanced to 80°bTDC or earlier the knock was appropriately suppressed, with sufficient time remaining for the additional fuel mass to mix into the end gas region. With later injection timings the knock intensity progressively increased, with average KI values as high as ~3bar but with some individual cycles exhibiting knock intensities of up to 12 bar at the latest injection timings studied. The excess fuel suppresses the knock via two well known mechanisms. Firstly, the charge cooling effect associated with evaporation of the fuel and secondly the reduced ratio of specific heats under richer conditions leading to lower end-gas temperatures after compression, as previously demonstrated in a real multi-cylinder DI engine [31]. However, it is important to note that auto-ignition delay times reduce under rich conditions, which arguably becomes more important when using excess fuel under severe knocking conditions as discussed in more detail below.

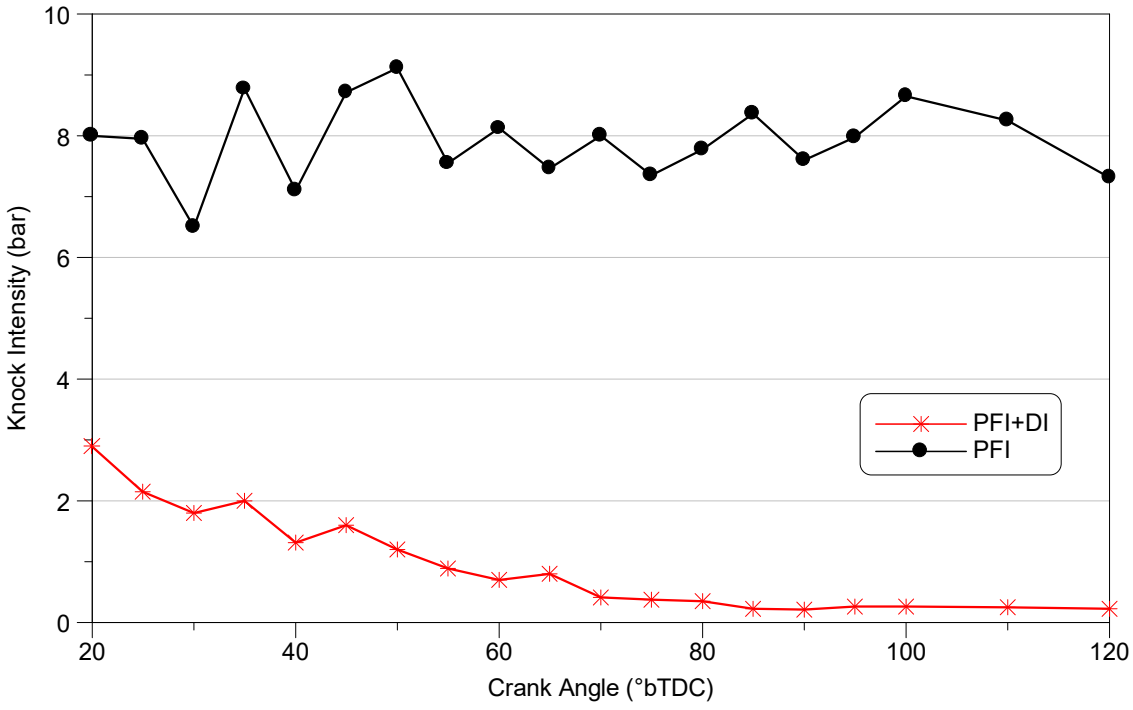


**Figure 4: Start of injection timing sweep under fixed DI pulse width and rail pressure**

Shown in Figure 5 are key thermodynamic values during the DI timing sweep. It should be acknowledged that the engine was operating at the stability limit under PFI only mode, due to the running conditions necessary to invoke heavy knock. As the direct injected fuel was introduced it can be seen that the stability fell below the COV of IMEP threshold; associated with advanced and faster combustion. In turn, the output of the engine increased. Clearly some stratification in the DI fuel was favorable to the mass burning rate and knock suppression, presumably due to preferential local conditions in the end-gas leading to lower temperature and/or prolonged auto-ignition delay. These observations appear to be in good agreement with those of Wang et al. [48], who employed split (double) direct injection to suppress Super-Knock in a modern downsized DI engine. However, some caution is required in this comparison as the exact mechanisms of Super-Knock suppression (i.e. stratification, reduced wall wetting) were unknown. In future work it is intended to study such effects under elevated injection pressures with different fuels.

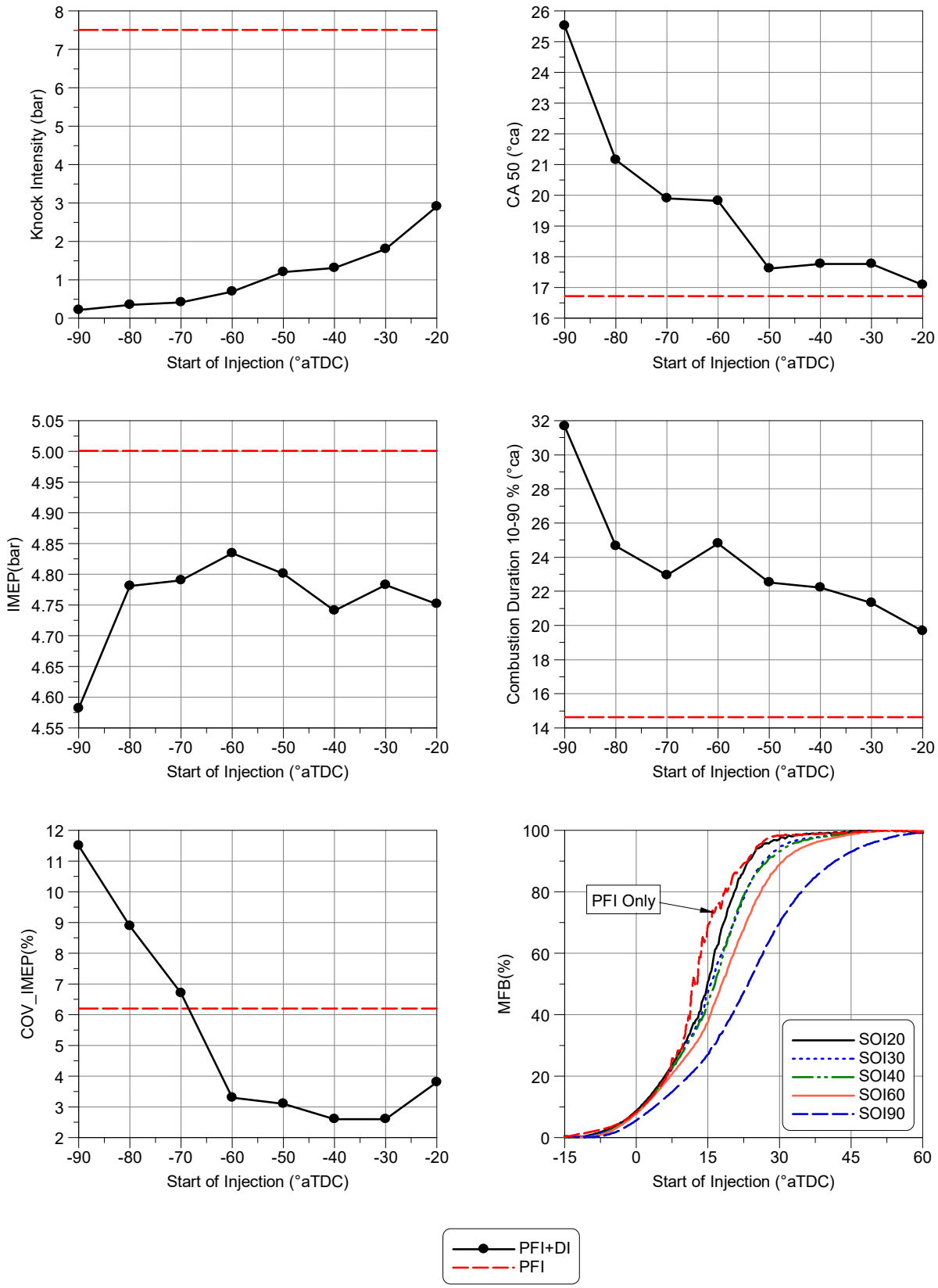


**Figure 5: Thermodynamic operating parameters during the SOI timing sweep**

### 3.2. Direct Fuel Injection Duration Sweep

A direct fuel injection duration sweep was undertaken to establish the response to increasing fuel mass, as might be experienced during real transient engine operation under knocking conditions. During the experiment the SOI timing was fixed at 60°bTDC and the fuel rail pressure set to 65 bar. All other parameters remained fixed as per Table 2. Set out in Figure 6 are the values of average knock intensity. Shown in Figure 7 are the corresponding measured values of relative air-to-fuel ratio (obtained via a wide band sensor fitted in the exhaust). In contradiction to the well-reported charge cooling and ratio of specific heat effects, it can be seen that with small additional DI fuel mass the knock intensity increased by ~65% at 1.5ms. It should also be noted that this was not associated with increasing engine torque, as the load reduced marginally throughout the sweep, steadily falling from 5.1bar (PFI-only) to 4.7bar IMEP at the richest condition. The increasing knock intensity has been associated with reducing auto-ignition delay times under rich conditions, which under heavy knock with low additional fuel mass outweighs the charge cooling and reduction in ratio of specific heats.

This observation was validated by reviewing the auto-ignition delay times for the two components of the fuels, with an example set out in Figure 8. This figure has been directly reproduced from recent simulation work by Stapf and Reis [17], where the solid lines denote their own predictions and the data points experimental shock tube measurements made elsewhere [21-22]. The predictions were determined using a simple Livengood-Wu integral model linked to a zero-dimensional engine code fed with experimental in-cylinder pressure. For both primary reference fuel components there is good agreement between the simulated and experimental results and that the auto-ignition delay time reduces under richer operating conditions (notably more so in the case of n-heptane).

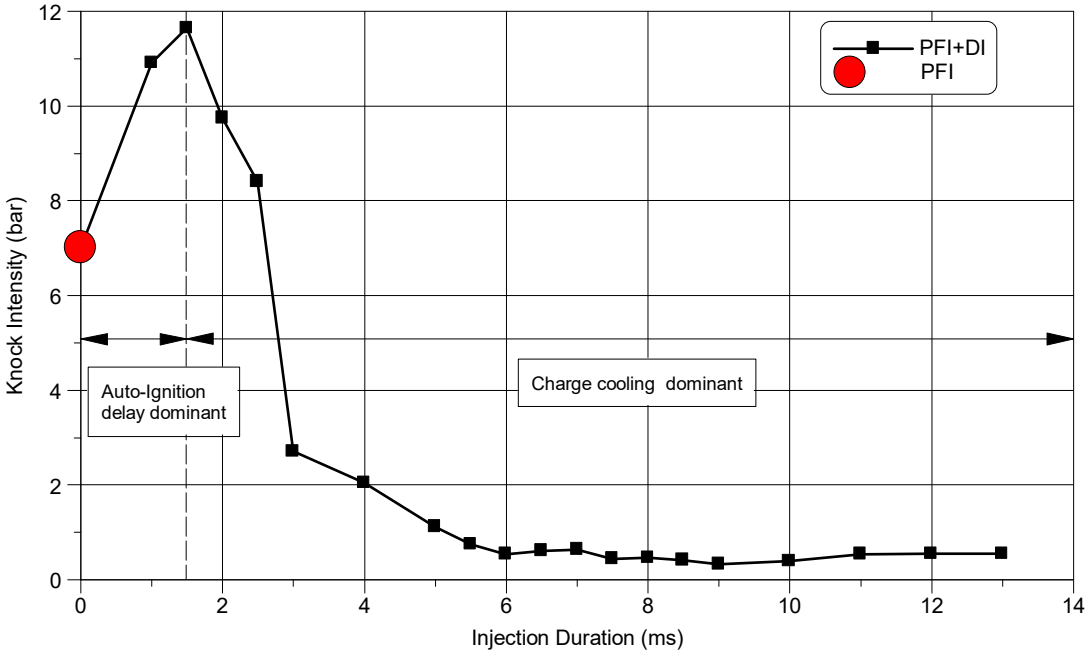


Figure 6: Average knock intensity versus direct fuel injection duration

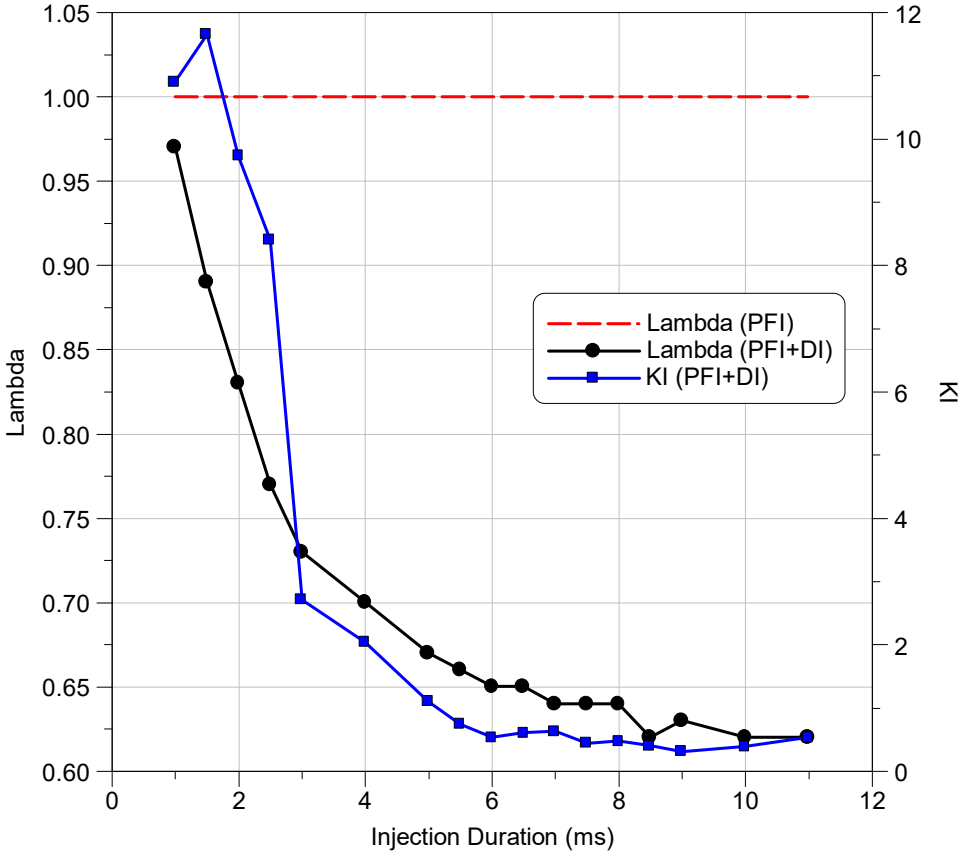


Figure 7: Injection Duration Sweep for different cycles during the PFI + DI with the average superimposed

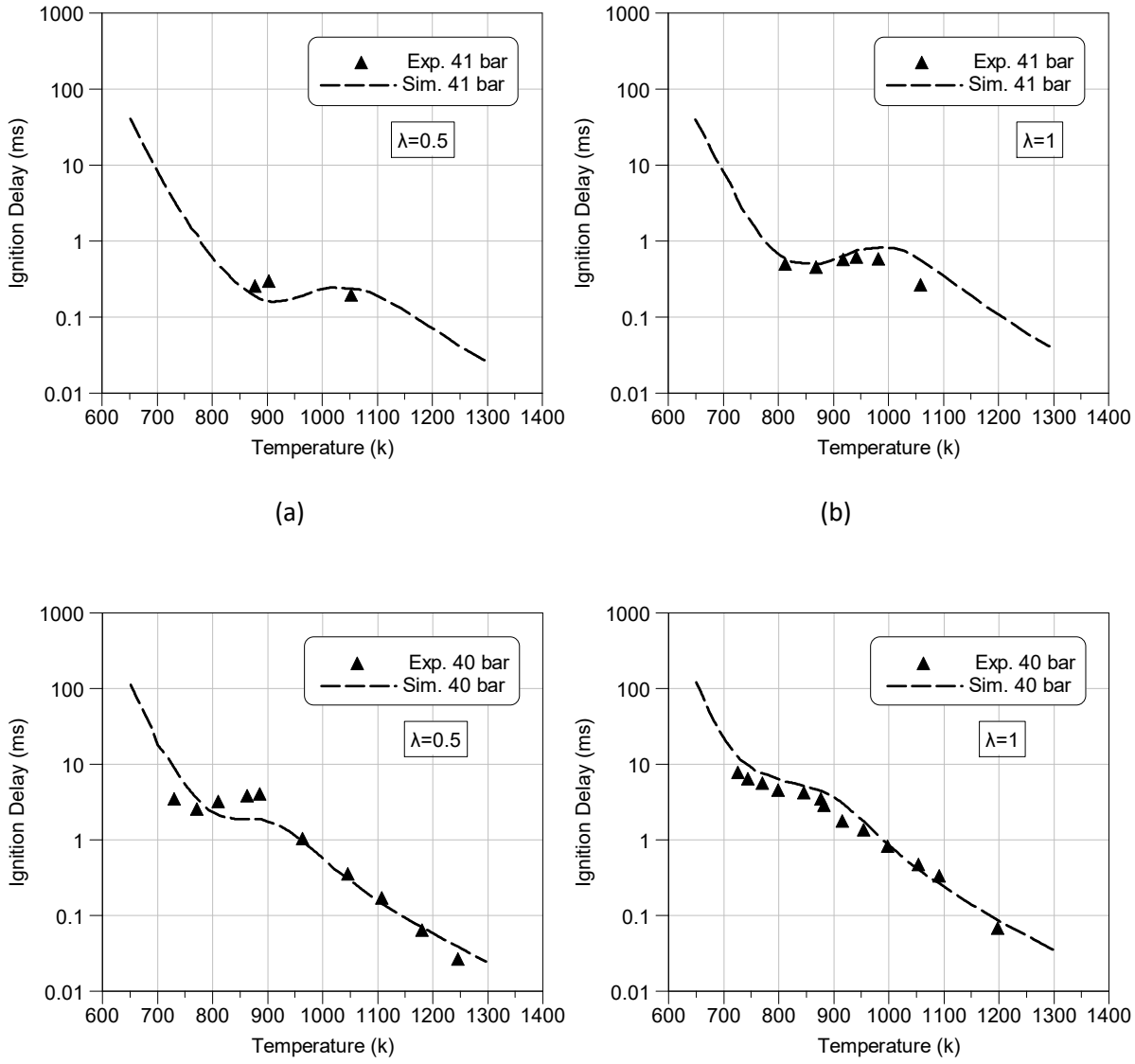


**Figure 8: Predictions and measurements of auto-ignition delay versus gas temperature for iso-octane under a) rich and b) stoichiometric conditions compared to equivalent values for n-heptane (c, d). Reproduced from [17].**

## 4. Optical Analysis

Shown in Figure 9 are flame images from three cycles selected to show "typical" events under varied start of injection timings. Each horizontal strip denotes a different cycle and SOI setting, as marked on the figure. As before, the fuel injection pulse width and DI rail pressure remained fixed at 7ms and 65bar respectively. All other test conditions remained fixed as identified previously in Table 2. The bright yellow-ish light omission denotes local sooty combustion in the end-gas region, with the phenonenon exacerbated as the DI timing was retarded. Set out in Figure 10 are corresponding flame image strips showing the "optimum" PFI+DI case versus PFI-only (with the flame images shown in the same orientation as Figure 9). Based on the previous results, the optimum direct injection timing was considered to be 60°bTDC. The corresponding in-cylinder pressure traces and mass fraction burned profiles are set out in Figures 11 and 12 and respectively. Under knocking conditions the mass fraction burned computation becomes unreliable after the peak in-cylinder pressure is attained. When the excess fuel was introduced it can be seen that the knock was entirely eliminated, with prolonged combustion duration, significantly lower peak in-cylinder pressure and higher gas pressures during the power stroke.

Shown in Figure 13 is a zoomed-in view of the single frame at 22.8°aTDC for the baseline PFI-only cycle first shown in Figure 10, where multiple-centred knock initiation sites were captured. The contrast in this frame has been manipulated for improved clarity. Such multiple centres were regularly noted under heavy knocking conditions, in good agreement with prior developing detonation theory [11-13, 23]. Under the rich PFI+DI conditions, in Figure 10 the flame can be seen to propagate rapidly downward toward the direct injector, with an apparent peninsular of flame growth in the bottom left-hand area of the bore potentially associated with favourable local mixutre strength. This phenomenon was regularly observed under these optimum settings. Overall, increased chemiluminescence was observed throughout the PFI+DI flame propagation event,

indicating some of the DI fuel had reached the region the spark plug region of the bore due to the (relatively) earlier direct injection timing. It was also interesting to note the area of negative flame curvature in the area of the original flame closest to the auto-ignition sites, where the new kernel(s) in the end gas presumably opposed the propagation of the original flame. Such negative curvature was regularly observed during similar cycles and was detrimental to the entrainment of the remaining unburned mass prior to the violent end-gas auto-ignition.

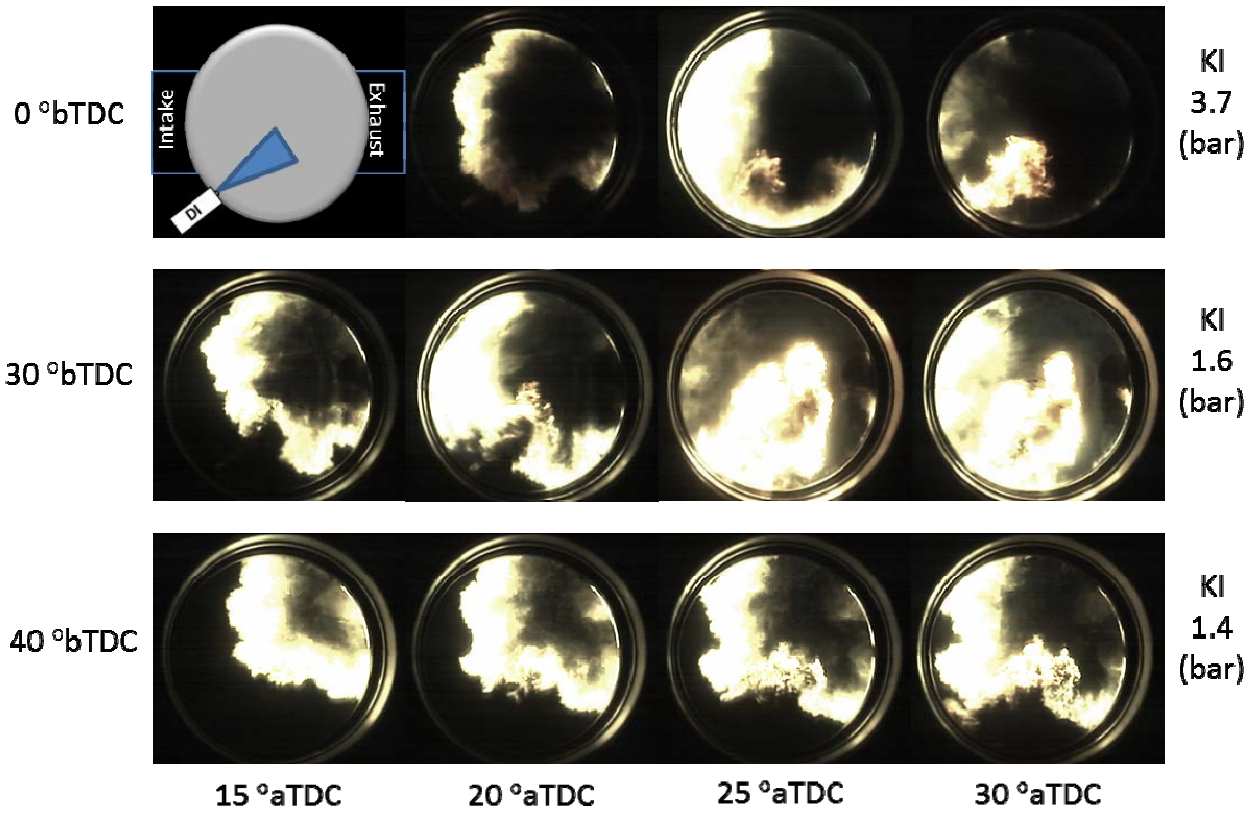


**Figure 9: Flame images under varied direct injection SOI timings. Each horizontal strip shows a different cycle obtained at different DI SOI timing (marked on the left).**

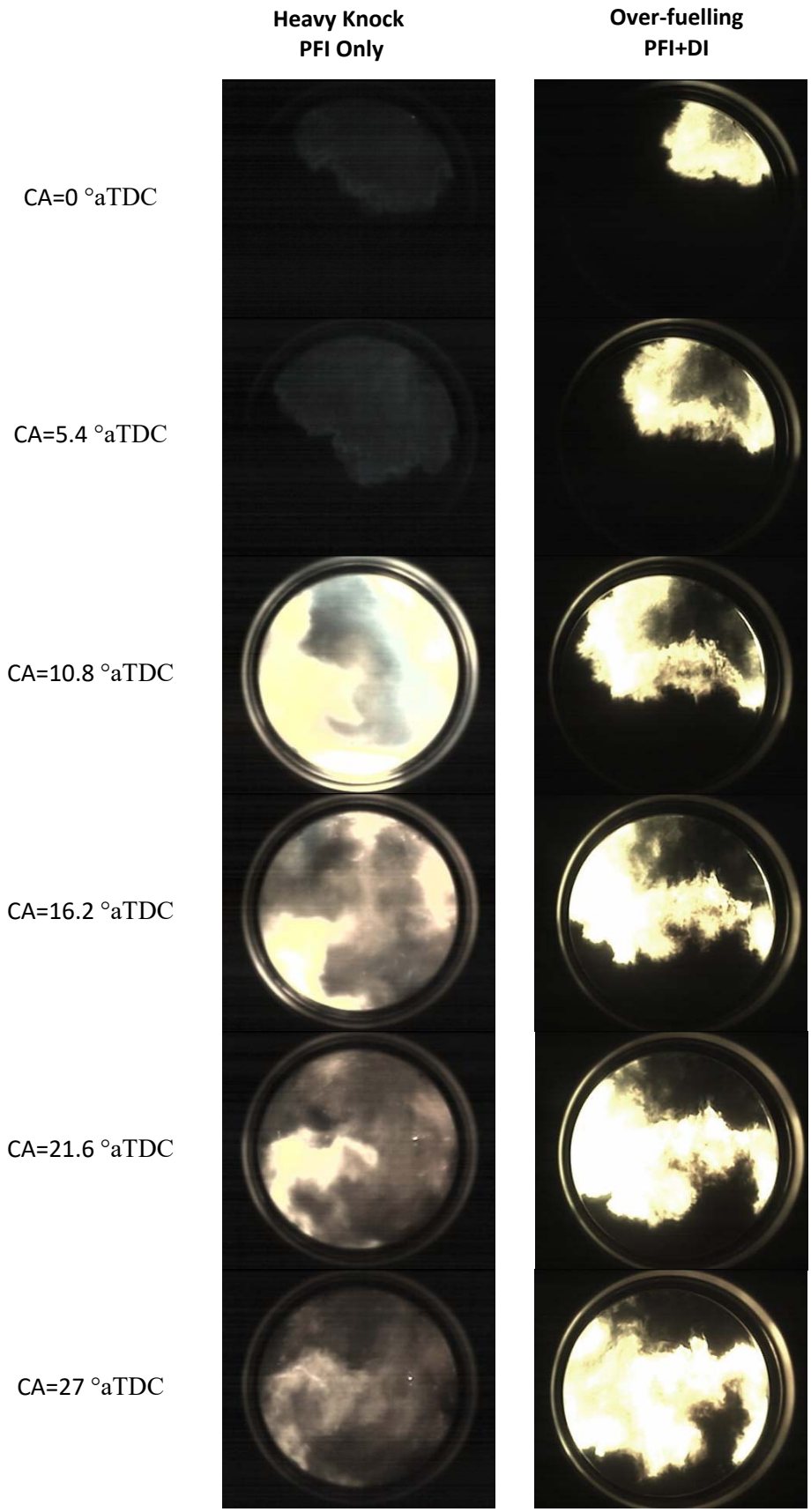


**Figure 10: A comparison of a typical baseline heavy knocking cycle versus a typical "optimum" over-fuelling cycle**

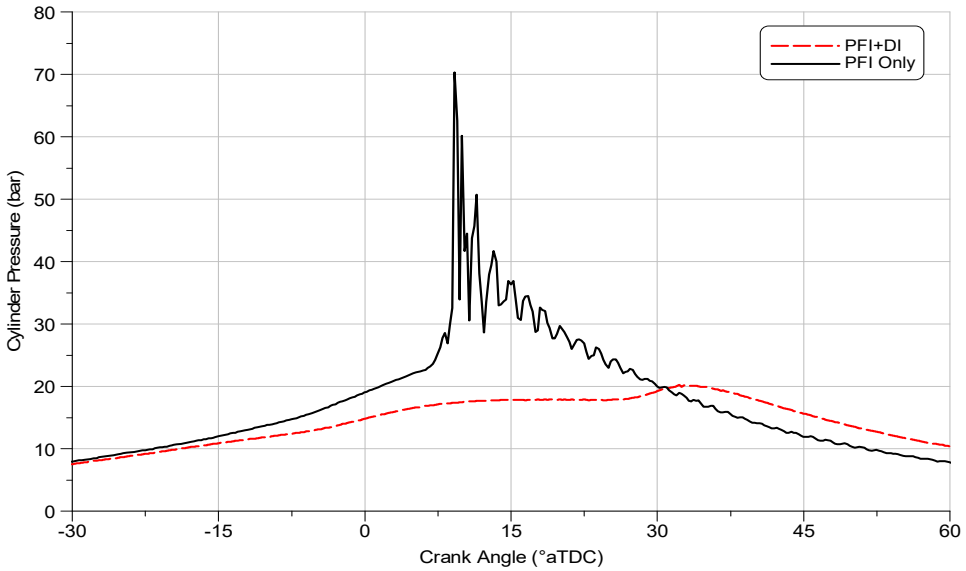


**Figure 11: Individual cycle in-cylinder pressure traces for the two optical cycles**

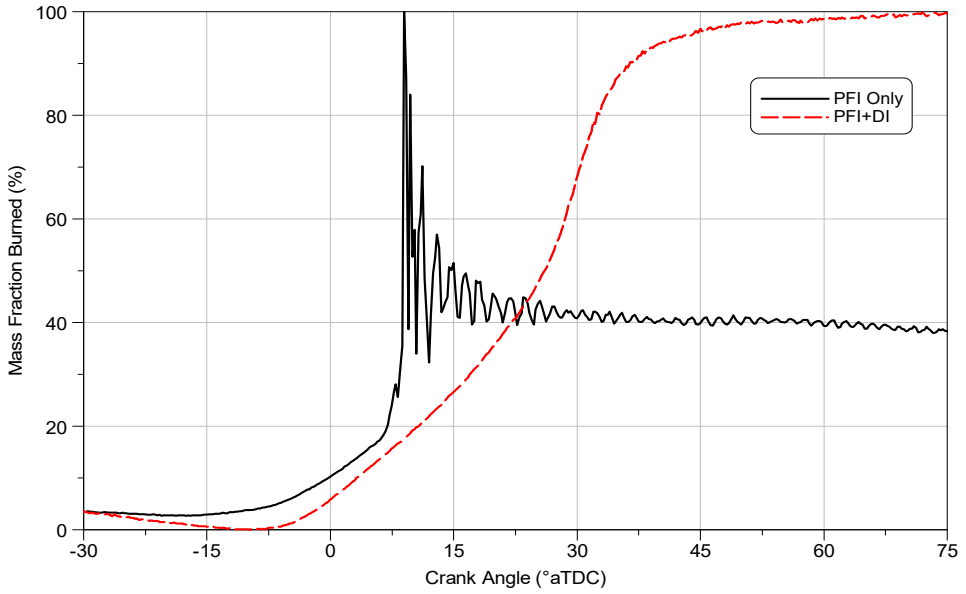


**Figure 12: Mass fraction burned profiles for the two optical cycles**

**Figure 13: Blown-up intensified view of the multiple auto-ignition initiation sites observed during the baseline heavy knock cycle shown in Figure 10**

## 5. CONCLUSIONS

The work involved study of transient over-fuelling using additional direct fuel injection during heavy knocking PFI engine conditions. It was observed that directly injecting a small-to-moderate additional mass of fuel would exacerbate knock, with reducing auto-ignition delay time leading to higher peak in-cylinder pressures and knock intensities elevated by ~65%. As the additional mass of excess fuel was further increased, the effects of charge cooling and reducing ratio of specific heats began to dominate and ultimately eliminated knock, albeit requiring extremely rich conditions. It was also apparent that some stratification in the fuel-air charge was favorable to burning rate and knock suppression, associated with favorable local conditions in the end gas prior to the onset of auto-ignition. Full bore chemiluminescence imaging confirmed multiple centred auto-ignition sites

and the need to balance the degree of pre-mixing of the excess fuel within the main charge, with increased light emission noted across the bore under the “optimum” DI conditions.

During heavy knocking conditions it was also interesting to note the area of negative flame curvature in the area of the original flame closest to the auto-ignition sites, where the propagation of new kernel(s) in the end gas opposed the expansion of the original flame. Such negative curvature was regularly observed and was detrimental to the entrainment of the remaining unburned mass prior to violent end-gas auto-ignition.

Overall, the results highlight the potential risks in transient over-fuelling under heavy knocking conditions, where an unexpected violent knocking event (e.g. Super-Knock) might be exacerbated by the presence of excess fuel leading to reduced auto-ignition delay. The observations demonstrate that traditional over-fuelling may be an unreliable method of super-knock suppression in modern downsized spark ignition engines, even without considering the other detrimental effects of rich combustion on thermal efficiency and tailpipe pollutant emissions. However, some caution is recommended given the simple nature of the fuels adopted and future work will consider the effects of a wider suite of fuels.

## 6. REFERENCES:


[1] Cairns, A., Stansfield, P., Fraser, N., Blaxill, H., Gold, M., Rogerson, J., and Goodfellow, C., "A Study of Gasoline-Alcohol Blended Fuels in an Advanced Turbocharged DISI Engine," Society of Automotive Engineers (SAE) International Journal of Fuels and Lubricants 2009-01-0138, (2009)

[2] Gröger, O., Gasteiger, H.A., and Suchsland, J.-P.: "Review—Electromobility: Batteries or Fuel Cells?,", Journal of the Electrochemical Society, 162(14):A2605–A2622, (2015)

[3] Moxey, B.G., Cairns, A., and Zhao, H., "A comparison of butanol and ethanol flame development in an optical spark ignition engine", Fuel, Volume 170, pp. 27-38, (2016)

[4] Cairns, A. , Zhao, H. , Todd, A. and Aleiferis, P.: "A study of mechanical variable valve operation with gasoline-alcohol fuels in a spark ignition engine", Fuel, 106 pp. 802 - 813, (2013)

[5] Turner, J.W.G., Pearson, R.J., Dekker, E., Iosefa, B., Johansson, K., Bergstrom, K.: "Extending the role of alcohols as transport fuels using iso-stoichiometric ternary blends of gasoline, ethanol and methanol", Applied Energy, 102 (2013), pp. 72–86, (2013)

[6] Lumsden, G., OudeNijeweme, D., Fraser, N., and Blaxill, H., "Development of a Turbocharged Direct Injection Downsizing Demonstrator Engine," SAE International Journal of Engines, 2(1):1420–1432, (2009)

[7] Ricardo, H.:"The High-Speed Internal-Combustion Engine", Blackie & Son Ltd., (1931)

[8] Zhen, X., Wang, Y., Xu, S., Zhu, Y., Tao, C., Xu, T., Song, M.:"The Engine Knock Analysis - An Overview", Applied Energy, 92 pp.628-636, (2012)

[9] Bozza, F., De Bellis, V., Teodosio, L.: "Potentials of Cooled EGR and Water Injection for Knock Resistance and Fuel Consumption Improvements of Gasoline Engines", Applied Energy, 169 pp112-125, (2016)

[10] De Bellis, V.: "Performance Optimisation of a Spark Ignition Turbocharged VVA Engine Under Knock Limited Operation", Applied Energy 164 pp162-174, (2016)

[11] König, G., Maly, R.R., Bradley, D., Lau, a K.C., and Sheppard, C.G.W., "Role of Exothermic Centres on Knock Initiation and Knock Damage" SAE Technical Paper 902136, (1990)

[12] Pan, J. and Sheppard, C.G.W., "A Theoretical and Experimental Study of the Modes of End Gas Autoignition Leading to Knock in S. I. Engines," SAE Technical Paper 942060, (1994)

[13] Pan, J., Sheppard, C.G.W., Tindall, A., Berzins, M., Pennington, S. V., and Ware, J.M., "End Gas Inhomogeneity, Autoignition and Knock," SAE Technical Paper 982616, (1998)

[14] Dahnz, C., Han, K.-M., Spicher, U., Magar, M., Schiessl, R., and Maas, U., "Investigations on Pre-Ignition in Highly Supercharged SI Engines," SAE International Journal of Engines, 3(1):214–224, (2010)

[15] Misdariis, A., Vermorel, O., Poinsot, T.: "A methodology based on reduced schemes to compute autoignition and propagation in internal combustion engines", Proceedings of the Combustion Institute, 35 (3), pp. 3001-3008., (2015)

[16] Pan, J., Shu, G., Zhao, P., Wei, H., Chen, Z.: "Interactions of flame propagation, auto-ignition and pressure wave during knocking combustion", Combustion and Flame, 164, pp. 319-328., (2016)

[17] Stapf, K. and Reis, B.: "Simulation of Auto-Ignition Behaviour for Varying Gasoline Engine Operating Conditions", Proceedings of the 2nd Conference on Engine Processes, July 02-03, Berlin, (2015).

[18] Haiqiao Wei, Yibao Shang, Ceyuan Chen, Dongzhi Gao, Dengquan Feng, "A numerical study on pressure wave-induced end gas auto-ignition near top dead center of a downsized spark ignition engine", International Journal of Hydrogen Energy, Volume 39, Issue 36, (2014)

[19] Yu, H., Chen, Z., "End-gas autoignition and detonation development in a closed chamber", Combustion and Flame, 162 (11), pp. 4102-4111, (2015)

[20] Ma, J., Kwak, K.H., Lee, B., Jung, D.: "An empirical modeling approach for the ignition delay of fuel blends based on the molar fractions of fuel components", FUEL, 164, pp. 305-313, (2016)

[21] Fieweger, K., Blumenthal, R., Adomeit, G.: "Self Ignition of SI Engine Model Fuels: A Shock Tube Investigation at High Pressure", Combustion and Flame 109, (1997).

[22] Ciezk, H., Adomeit, G.: "Shock tube investigation of n-heptane air mixtures under engine relevant conditions", Combustion and Flame 93, (1993).

[23] Kalghatgi, G.T. and Bradley, D., “Pre-ignition and ‘super-knock’ in turbo-charged spark-ignition engines,” International Journal of Engine Research, 13(4):399–414, (2012)

[24] Peters, N. and Kerschgens, B., “Super-Knock Prediction Using a Refined Theory of Turbulence,” SAE International Journal of Engines, 6:953–967, (2013)

[25] Bates, L., Bradley, D., Paczko, G. and Peters, N.: "Engine hot spots: Modes of auto-ignition and reaction propagation", Combustion and Flame, (2016)

[26] Wang, Z., Qi, Y., He, X., Wang, J., Shuai, S., Law, C.K.: "Analysis of pre-ignition to super-knock: Hotspot-induced deflagration to detonation", Fuel, 144, pp. 222-227, (2015)

[27] Amann M, Alger T, Westmoreland B, Rothmaier A.: "The Effects of Piston Crevices and Injection Strategy on Low-Speed Pre-Ignition in Boosted SI Engines", SAE International Journal of Engines; 5:1216–28. doi:10.4271/2012-01-1148, (2012)

[28] Griffiths, J.G., MacNamara, J.P., Sheppard, C.G.W., Turton, D.A., Whitaker, B.J.:"The relationship of knock during controlled autoignition to temperature inhomogeneities and fuel reactivity", Fuel, 81 pp.2219-2225, (2002)

[29] Dingle, S.F., Cairns, A., Zhao, H., Williams, J., Williams, O., and Ali, R., “Lubricant Induced Pre-Ignition in an Optical SI Engine,” SAE Technical Paper 2014-01-1222, (2014)

[30] Welling, O., Moss, J., Williams, J., and Collings, N., "Measuring the Impact of Engine Oils and Fuels on Low-Speed Pre-Ignition in Downsized Engines," *SAE Int. J. Fuels Lubr.* 7(1):1-8, doi:10.4271/2014-01-1219, (2014)

[31] Cairns, A., Fraser, N., and Blaxill, H., "Pre Versus Post Compressor Supply of Cooled EGR for Full Load Fuel Economy in Turbocharged Gasoline Engines," SAE Technical Paper 2008-01-0425, (2008)

[32] Nose, H., Inoue, T., Katagiri, S., Sakai, A. et al., "Fuel Enrichment Control System by Catalyst Temperature Estimation to Enable Frequent Stoichiometric Operation at High Engine Speed/Load Condition," SAE Technical Paper 2013-01-0341, doi:10.4271/2013-01-0341, (2013)

[33] Zhao, H. “Advanced Direct Injection Combustion Engine Technologies and Development,”, Woodhead Publishing, (2009)

[34] Zhuang, Y. and Hong, G.: "Effects of Direct Injection Timing of Ethanol Fuel on Engine Knock and Lean Burn in a Port Injection Gasoline Engine", Fuel 135 pp.27-37, (2014)

[35] Rothamer, D. and Jennings, J.: "Study of the Knocking Propensity of 2,5 dimethylfuran-gasoline and ethanol-gasoline blends", Fuel, 98 pp.203-212, (2012)

[36] Hamilton, L., Rostedt, M., Caton, P., and Cowart, J., "Pre-Ignition Characteristics of Ethanol and E85 in a Spark Ignition Engine," *SAE Int. J. Fuels Lubr.* 1(1):145-154, (2009)

[37] König, G., Maly, R., Bradley, D., Lau, A. et al., "Role of Exothermic Centres on Knock Initiation and Knock Damage," SAE Technical Paper 902136, (1990)

[38] Yang, C.-H., Zhao, H.: "In-cylinder studies of hybrid combustion in a direct injection single-cylinder optical engine", International Journal of Engine Research, 11 (6), pp. 515-531, (2010)

[39] Breda, S., D'Adamo, A., Fontanesi, S., Giovannoni, N. et al., "CFD Analysis of Combustion and Knock in an Optically Accessible GDI Engine," *SAE Int. J. Engines* 9(1):641-656,

(2016)

[40] Tinaut, F.V., Reyes, M., Giménez, B., Pastor, J.V.: "Measurements of OH* and CH* chemiluminescence in premixed flames in a constant volume combustion bomb under autoignition conditions", Energy and Fuels, 25 (1), pp. 119-129, (2011)

[41] Aleiferis, P. and Rosati, M.:"Controlled autoignition of hydrogen in a direct injection optical engine", Combustion and Flame, Vol 159, Issue 7, (2012)

[42] Merola, S., Valentino, G., Tornatore, C., Marchitto, L.: "In-cylinder spectroscopic measurements of knocking combustion in a SI engine fuelled with butanol-gasoline blend", Energy, Vol 62, pp 150-161, (2013)

[43] Kawahara, N., Tomita, E.: "Visualisation of auto-ignition and pressure wave during knocking in a hydrogen SI engine", International Journal of Hydrogen Energy, Vol 34, Issue 7, pp 3156-3163, (2009)

[44] Geiser, F., Wytrykus, F., and Spicher, U., "Combustion Control with the Optical Fibre Fitted Production Spark Plug," SAE Technical Paper 980139, (1998)

[45] Magar, M., Spicher, U., Palaveev, S., Gohl, M. et al., "Experimental Studies on the Occurrence of Low-Speed Pre-Ignition in Turbocharged GDI Engines," *SAE Int. J. Engines* 8(2):495-504, (2015)

[46] Rassweiler, G.M. and Withrow, L., “Motion Pictures of Engine Flames Correlated with Pressure Cards,” SAE Technical Paper 1938-01-01, (1938).

[47] Knop, V. and Essayem, E., “Comparison of PFI and DI Operation in a Downsized Gasoline Engine,” SAE Int. J. Engines 6(2):941–952, (2013).

[48] Wang, Z., Liu, H., Song, T., Xu, Y. et al., "Investigation on Pre-ignition and Super-Knock in Highly Boosted Gasoline Direct Injection Engines," SAE Technical Paper 2014-01-1212, (2014).

**ACRONYMS**

**aTDC:** after Top Dead Centre

**AFR:** Air-to-Fuel Ratio

**bTDC:** before Top Dead Centre

**BMEP:** Brake Mean Effective Pressure

**BSFC:** Brake Specific Fuel Consumption

**CA:** Crank Angle

**CCV:** Cycle-by-Cycle Variation

**COV:** Coefficient of Variation

**DI:** Direct Injection

**EU:** European Union

**ID:** Injection Duration

**IDS:** Injection Duration Sweep

**IMEP:** Net Indicated Mean Effective Pressure

**MFB:** Mass Fraction Burned

**NEDC:** New European Drive Cycle

**PFI:** Port Fuel Injection

**RON:** Research Octane Number

**SOI:** Start of Injection

**SOIS:** Start of Injection Sweep

**SI:** Spark Ignition

**TDC:** Top Dead Centre

**VVT:** Variable Valve Timing

**WOT:** Wide Open Throttle

**λ:** Relative air-to-fuel ratio

**APPENDICES:**

## APPENDIX A: FUEL PROPERTIES

| **Property** | **Iso-Octane** | **n-Heptane** |
|---|---|---|
| Chemical Formula | C8H18 | C7H16 |
| Boiling point at 1 atm (°c) | 99.2 | 98.4 |
| Enthalpy of vaporisation at 298.15 K (MJ/Kmol) | 35.14 | 36.63 |
| Density at 25°C ($Kg/m^3$) | 690.4 | 681.5 |
| Latent Heat of Vaporisation(kJ/kg) | 308 | 318 |
| Reid Vapour Pressure (bar) | 0.52 | 0.12 |
| Oxygen Content by Weight (%) | 0 | 0 |
| Volumetric Energy Content (MJ/l) | 30.6 | 30.48 |
| RON (MON) | 100 (100) | 0 (0) |

**Table A1: Primary reference fuel properties**

## APPENDIX B: EXPERIMENTAL SETUP

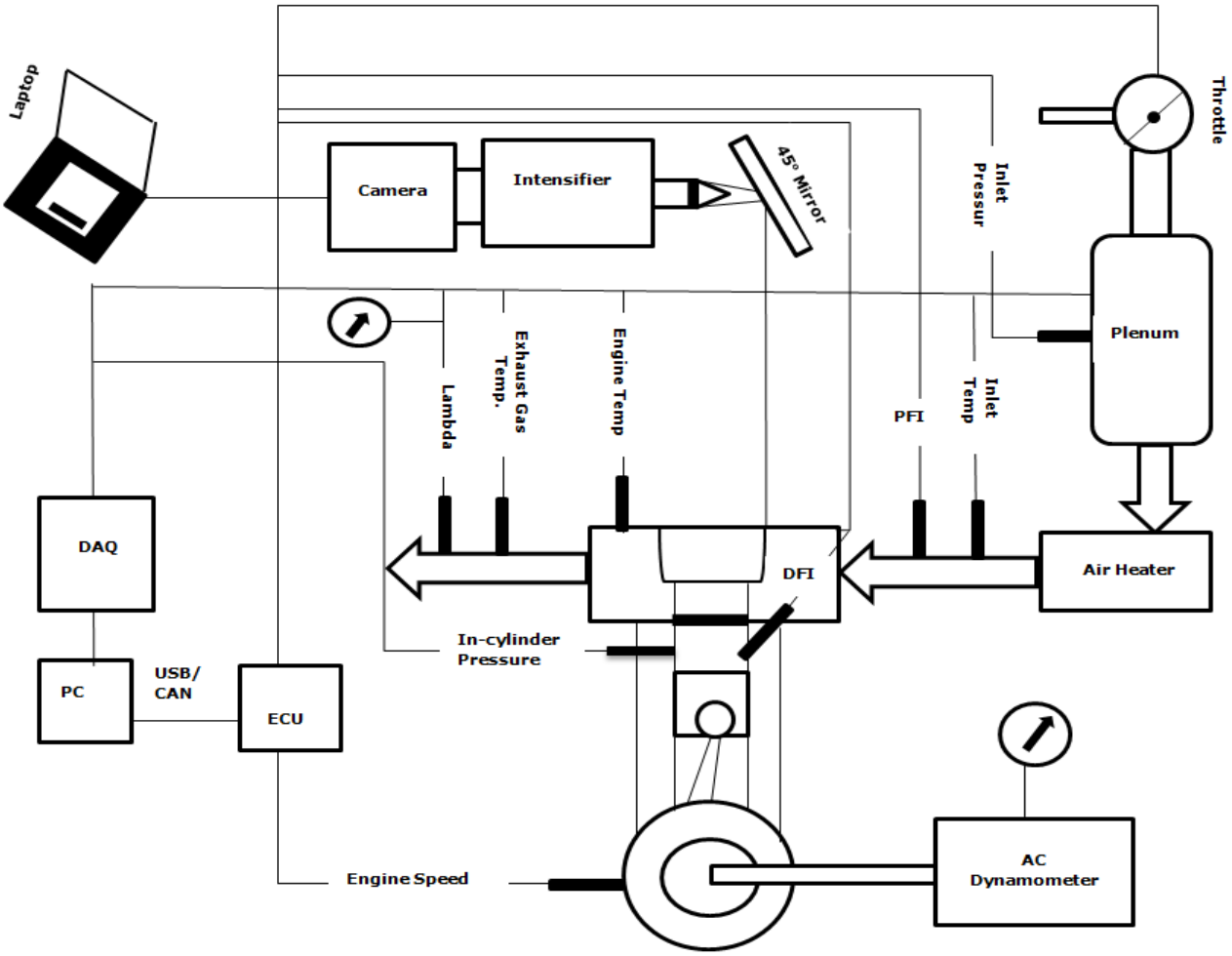


**Figure B1: Schematic of experimental engine control, image capture & data acquisition systems**